

Effect of Short-ranged Order on the electronic structure and optical properties of the CuZn alloy : an augmented space approach.

Kartick Tarafder,¹ Atis dipankar Chakrabarti ^{*,1} Kamal Krishna Saha,² and Abhijit Mookerjee¹

¹*S.N. Bose National Center for Basic Sciences, JD Block,
Sector III, Salt Lake City, Kolkata 700 098, India*

²*Theory Department, Max-Planck-Institut für Mikrostrukturphysik, Weinberg 2, D-06120 Halle (Saale), Germany*

(Dated: September 4, 2018)

We report here a study of the effect of short-ranged ordering on the electronic structure and optical properties of CuZn alloys. We shall use the augmented space recursion technique developed by us in conjunction with the tight-binding linear muffin tin orbitals basis.

PACS numbers: 75.50.Pp

INTRODUCTION

Binary alloys involving equal proportions of a noble metal Cu and a divalent metal Zn have a stable low temperature β -phase which sits immediately to the right of the pure face-centered cubic Cu phase in the alloy phase diagram [1, 2]. This phase called β brass has a B2 cubic structure with two atoms per unit cell. At high temperatures the alloy forms a disordered body-centered cubic structure. The disorder-order transition takes place around 730K. The alloy satisfies the Hume-Rothery rules [3] and has the same ratio of valence electrons to atoms. Jona and Marcus [1] have shown from a Density Functional Theory (DFT) based approach that within the Local Density Approximation (LDA), it is the body-centered based B2 which is the stable ground state. They also showed that if we include the Gradient Corrections (GGA) then we get a tetragonal ground state lower in energy by 0.1 mRy/atom. This is in contradiction with the latest experimental data. The alloying of face-centered cubic Cu with an equal amount of Zn leads to a body-centered stable phase. Zn has only one more electron than Cu. This is an interesting phenomenon. CuZn alloys also have anomalously high elastic anisotropy. This makes the theoretical study of CuZn an interesting exercise for a proposed theoretical technique. The phase diagram of CuZn is shown in Fig. 1.

One of the earliest first-principles Density functional based study of the electronic properties of CuZn as by Bansil [4]. The authors had studied the complex bands of α -phase of CuZn using the Korringa-Kohn-Rostocker (KKR) method coupled with the coherent potential approximation (CPA) to take care of disorder. They commented on the effects of charge transfer and lattice constants on the electronic structure. They found the elec-

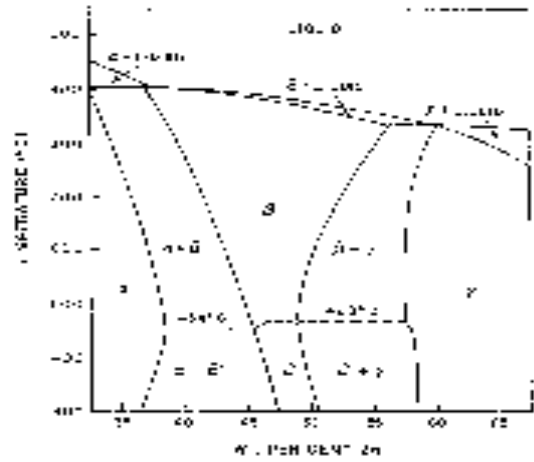


FIG. 1: Experimental phase diagram of CuZn alloy

tronic distribution of this alloy to be of a split band kind with the centers of the Cu and Zn d -bands well separated from each other. Their Zn d -bands showed hardly any dispersion and were shown only schematically in their figures. In a later work Rowlands [5] generalized the CPA to a non-local version (NL-CPA) and studied the effects of short-ranged ordering in CuZn. Their technique was based on an idea of renormalization in reciprocal space suggested by Jarrel and Krishnamurthy [6].

The order-disorder transition in CuZn is a classical example of a true second order transition. Several very early investigations on this alloy has been reviewed by Nix and Shockley [7] and Guttman [8]. These investigations, of course, were rather crude, as sophisticated approaches to deal with disordered alloys had not really been developed at that time. However, it was recognized that a knowledge of the short-ranged order correlations above the critical temperature should be of considerable interest. Early neutron scattering experiments were carried out on β -brass by Walker and Keating [9]. The

*Permanent address : Ramakrishna Mission Vivekananda Centenary College, Rahara, West Bengal, India

Warren-Cowley short-ranged order parameter, defined by $\alpha(R) = 1 - P_{AB}(R)/x$ where x is the concentration of A, $P_{AB}(R)$ is the probability of finding an A atom at a distance of R from a B atom, was directly obtained from the diffuse scattering cross-section :

$$\frac{d\sigma}{d\Omega} = x(1-x)(b_A - b_B)^2 \sum_R \alpha(R) f(K) \exp(iK \cdot R)$$

where b_A, b_B are the scattering lengths of A and B atoms, and $f(K) = \exp(-C|K|^2)$ is the attenuation factor arising from thermal vibrations and static strains. The experimental data for the short-ranged order parameter as a function of temperature are thus available to us. A Ising-like model using pair interactions was studied by Walker and Chipman [10] and the short-ranged order was theoretically obtained. However, the pair interactions were simply fitted to the experimental values of the transition temperature T_C and in that sense it was an empirical theory. The experimental estimate of the nearest neighbour Warren-Cowley parameter was found to be varying between -0.171 to -0.182 at around 750K.

In a later work using the much more sophisticated *locally self-consistent Green function* (LSGF) approach based on the tight-binding linear muffin-tin orbital (TB-LMTO) technique Abrikosov *et.al.* [11] studied CuZn alloys. The authors argued that earlier studies of the mixing enthalpies of CuZn using the standard coherent potential approximation approaches [12]-[16] showed significant discrepancy with experiment. Part of the discrepancy was assumed to be from neglect of charge transfer effects and part from the effects of short ranged ordering (SRO). The main thrust of this technique, which was based on an earlier idea of a locally self-consistent multiple scattering (LSMS) by Wang *et.al.* [17], was to go beyond the CPA and include the effects of the immediate environment of an atom in the solid. The LSMS gave an excellent theoretical estimate of the ordering energy in CuZn : 3.37 MRy/atom as compared to the experimental value of 3.5 MRy/atom. The LSGF approach correctly predicted ordering tendency in CuZn on lowering temperature and combining with a Cluster Variation Connolly Williams (CVM-CW) obtained a value of the nearest neighbour Warren-Cowley SRO parameter $\alpha = -0.15$. Subsequently Bruno *et.al.* [18] proposed a modification of the CPA taking into account the local field and showed that charge transfer effects can be taken into account accurately as compared to the O(N) methods just described. They applied their approach to the CuZn alloys.

One of the earlier works on the optical property of CuZn alloy was the determination of the temperature variation of spectral reflectivity by Muldawer [19]. The author attempted to explain the color of the disordered β -brass CuZn alloy via the internal photoelectric effect [20]. Al-

though, the experimental data also contained the contribution from plasma oscillations, the author claimed that the spectral reflectivity helps to explain the band picture of the alloys as a function of the inter-atomic spacing. In order to explain the optical properties, Amar *et.al.* [21]-[23] studied the band structure of CuZn using the KKR method. However, they had used the virtual crystal approximation, replacing the random potential seen by the electrons by an averaged one. This is now known to be particularly inaccurate for split band alloys.

The above discussion was necessary to bring into focus the following points : in the study of alloys like CuZn it would be interesting to address the effects of charge transfer and short-ranged ordering. In this communication we shall address exactly these two points. We shall propose the use of the augmented space recursion (ASR) coupled with the tight-binding linear muffin-tin orbitals basis (TB-LMTO) [24] to study the effects of short-ranged ordering on both the electronic structure and the optical properties of β -CuZn alloy at 50-50 composition. We should like to stress here that the TB-LMTO-ASR addresses precisely these effects with accuracy : the Density functional self-consistent TB-LMTO takes care of the charge transfer, while the local environmental effects which are essential for the description of SRO are dealt with by the ASR. The TB-LMTO-ASR and its advantages has been extensively discussed earlier by Mookerjee [25] and in a series of articles [24, 26, 27, 28, 29, 30]. We would like to refer the interested readers to these for details.

SPECTRAL FUNCTIONS, COMPLEX BANDS AND DENSITY OF STATES FOR 50-50 CUZN

In this section we shall introduce the salient features of the ASR which will be required by us in our subsequent discussions.

We shall start from a first principle TB-LMTO set of orbitals [31, 32] in the most-localized α representation. This is necessary, because the subsequent recursion requires a sparse representation of the Hamiltonian. In this representation, the second order alloy Hamiltonian is given by,

$$\mathbf{H}^{(2)} = \mathbf{E}_\nu + \mathbf{h} - \mathbf{h}\mathbf{h}$$

where,

$$\begin{aligned} \mathbf{h} &= \sum_R (\mathbf{C}_R - \mathbf{E}_{\nu R}) \mathcal{P}_R + \sum_R \sum_{R'} \Delta_R^{1/2} \mathbf{S}_{RR'} \Delta_{R'}^{1/2} \mathcal{T}_{RR'} \\ \mathbf{o} &= \sum_R \mathbf{o}_R \mathcal{P}_R \end{aligned} \quad (1)$$

\mathbf{C}_R , $\mathbf{E}_{\nu R}$, Δ_R and \mathbf{o}_R are diagonal matrices in angular momentum space, and $\mathbf{S}_{RR'}$ is the structure matrix. These matrices are of rank L_{max} . $\mathcal{P}_R = |R\rangle\langle R|$ and $\mathcal{T}_{RR'} = |R\rangle\langle R'|$ are projection and transfer operators in the Hilbert space \mathcal{H} spanned by the tight-binding basis $\{|R\rangle\}$. Here, R refers to the position of atoms in the solid and L is a composite label $\{\ell, m, m_s\}$ for the angular momentum quantum numbers. \mathbf{C} , Δ and \mathbf{o} are the potential parameters of the atoms which sit on the lattice sites ; \mathbf{o}^{-1} has dimension of energy and \mathbf{E}_{ν} 's are the reference energies about which the muffin-tin orbitals are linearized.

For a disordered binary alloy we may write :

$$\begin{aligned} C_{RL} &= C_L^A n_R + C_L^B (1 - n_R) \\ \Delta_{RL}^{1/2} &= (\Delta_L^A)^{1/2} n_R + (\Delta_L^B)^{1/2} (1 - n_R) \\ o_{RL} &= o_L^A n_R + o_L^B (1 - n_R) \end{aligned} \quad (2)$$

Here $\{n_R\}$ are the random site-occupation variables which take values 1 and 0 depending upon whether the muffin-tin labelled by R is occupied by an A or a B -type of atom. The atom sitting at $\{R\}$ can either be of type A ($n_R = 1$) with probability x or B ($n_R = 0$) with probability y , where x and y are the concentrations of the components A and B in the binary alloy. The augmented space formalism (ASF) now introduces the space of configurations of the set of binary random variables $\{n_R\} : \Phi$. In the absence of short-ranged order, each random variable n_R has associated with it an operator \mathbf{M}_R whose spectral density is its probability density :

$$\begin{aligned} p(n_R) &= x\delta(n_R - 1) + y\delta(n_R) \\ &= -\frac{1}{\pi} \lim_{\delta \rightarrow 0} \text{Im} \langle \uparrow_R | ((n_R + i\delta)\mathbf{I} - \mathbf{M}_R)^{-1} | \uparrow_R \rangle. \end{aligned} \quad (3)$$

\mathbf{M}_R is an operator whose eigenvalues 1, 0 correspond to the observed values of n_R and whose corresponding eigenvectors $\{|1_R\rangle, |0_R\rangle\}$ span a configuration space ϕ_R of rank 2. We may change the basis to $\{| \uparrow_R \rangle, | \downarrow_R \rangle\}$

$$\begin{aligned} | \uparrow_R \rangle &= \{\sqrt{x}|0_R\rangle + \sqrt{y}|1_R\rangle\} \\ | \downarrow_R \rangle &= \{\sqrt{y}|0_R\rangle - \sqrt{x}|1_R\rangle\} \end{aligned}$$

and in the new basis the operator \mathbf{M}_R corresponding to n_R is :

$$\begin{aligned} \mathbf{M}_R &= x\mathcal{P}_R^{\uparrow} + y\mathcal{P}_R^{\downarrow} + \sqrt{xy} \mathcal{T}_R^{\uparrow\downarrow} \\ &= x\mathcal{I} + b(x)\mathcal{P}_R^{\downarrow} + f(x)\mathcal{T}_R^{\uparrow\downarrow} \end{aligned}$$

where $\mathcal{P}_R^{\uparrow} = |\uparrow_R\rangle\langle \uparrow_R|$, $\mathcal{P}_R^{\downarrow} = |\downarrow_R\rangle\langle \downarrow_R|$ and $\mathcal{T}_R^{\uparrow\downarrow} = |\uparrow_R\rangle\langle \downarrow_R| + |\downarrow_R\rangle\langle \uparrow_R|$ are the projection and transfer operators in the configuration space ϕ_R spanned by the two basis vectors. $b(x) = (y - x)$ and $f(x) = \sqrt{xy}$.

The full configuration space $\Phi = \prod_R^{\otimes} \phi_R$ is then spanned by vectors of the form $|\uparrow\downarrow\uparrow\downarrow\dots\rangle$. These configurations may be labelled by the sequence of sites $\{\mathcal{C}\}$ at which we have a \downarrow . For example, for the state just quoted $\{\mathcal{C}\} = |\{3, 5, \dots\}\rangle$. This sequence is called the *cardinality sequence*. If we define the configuration $|\uparrow\uparrow\dots\uparrow\dots\rangle$ as the reference configuration, then the *cardinality sequence* of the reference configuration is the null sequence $\{\emptyset\}$.

In the full augmented space the operator corresponding to n_R is :

$$\widetilde{\mathbf{M}}_R = x\mathcal{I} \otimes \mathcal{I} \dots + b(x)\mathcal{P}_R^{\downarrow} \otimes \mathcal{I} \dots + f(x)\mathcal{T}_R^{\uparrow\downarrow} \otimes \mathcal{I} \dots \quad (4)$$

The augmented space theorem [26] states that

$$\ll A(\{n_R\}) \gg = \langle \{\emptyset\} | \widetilde{\mathbf{A}}(\{\mathbf{M}_R\}) | \{\emptyset\} \rangle, \quad (5)$$

where,

$$\widetilde{\mathbf{A}}(\{\widetilde{\mathbf{M}}_R\}) = \int \dots \int A(\{\lambda_R\}) \prod d\mathbf{P}(\lambda_R).$$

$\mathbf{P}(\lambda_R)$ is the spectral density of the self-adjoint operator $\widetilde{\mathbf{M}}_R$. Applying (5) to the Green function we get :

$$\ll \mathbf{G}(\mathbf{k}, z) \gg = \langle \mathbf{k} \otimes \{\emptyset\} | (z\widetilde{\mathbf{I}} - \widetilde{\mathbf{H}}^{(2)})^{-1} | \mathbf{k} \otimes \{\emptyset\} \rangle. \quad (6)$$

where \mathbf{G} and $\mathbf{H}^{(2)}$ are operators which are matrices in angular momentum space, and the augmented reciprocal space basis $|\mathbf{k}, L \otimes \{\emptyset\}\rangle$ has the form

$$(1/\sqrt{N}) \sum_R \exp(-i\mathbf{k} \cdot R) |R, L \otimes \{\emptyset\}\rangle.$$

The augmented space Hamiltonian $\widetilde{\mathbf{H}}^{(2)}$ is constructed from the TB-LMTO Hamiltonian $\mathbf{H}^{(2)}$ by replacing each random variable n_R by the operators $\widetilde{\mathbf{M}}_R$. It is an operator in the augmented space $\Psi = \mathcal{H} \otimes \Phi$. The ASF maps a disordered Hamiltonian described in a Hilbert space \mathcal{H} onto an ordered Hamiltonian in an enlarged space Ψ , where the space Ψ is constructed as the outer product of the space \mathcal{H} and configuration space Φ of the random variables of the disordered Hamiltonian. The configuration space Φ is of rank 2^N if there are N muffin-tin spheres in the system. Another way of looking at $\widetilde{\mathbf{H}}^{(2)}$ is to note that it is the *collection* of all possible Hamiltonians for all possible configurations of the system.

Combining (2) and (4) we get for any of the operators \mathbf{V} diagonal in real and angular momentum spaces :

$$\tilde{\mathbf{V}} = \sum_R \left\{ \mathbf{A}(\mathbf{V}) \mathcal{P}_R \otimes \mathcal{I} \otimes \mathcal{I} \dots + \mathbf{B}(\mathbf{V}) \mathcal{P}_R \otimes \mathcal{P}_R^\perp \otimes \mathcal{I} \dots + \mathbf{F}(\mathbf{V}) \mathcal{P}_R \otimes \mathcal{T}_R^{\uparrow\downarrow} \otimes \mathcal{I} \dots \right\} = \tilde{\mathbf{A}} + \tilde{\mathbf{B}} + \tilde{\mathbf{F}}. \quad (7)$$

where for any of the diagonal (in real and angular momentum spaces) operator \mathbf{V} :

$$\begin{aligned} \mathbf{A}(\mathbf{V}) &= (x V_L^A + y V_L^B) \delta_{LL'} \\ \mathbf{B}(\mathbf{V}) &= b(x)(V_L^A - V_L^B) \delta_{LL'} \\ \mathbf{F}(\mathbf{V}) &= f(x)(V_L^A - V_L^B) \delta_{LL'} \end{aligned} \quad (8)$$

In case there is no off-diagonal disorder due to local lattice distortion because of size mismatch :

$$\tilde{\mathbf{S}} = \sum_R \sum_{R'} \mathbf{A}(\Delta_R^{-1})^{-1/2} \mathbf{S}_{RR'} \mathbf{A}(\Delta_{R'}^{-1})^{-1/2} \mathcal{T}_{RR'} \otimes \mathcal{I} \otimes \mathcal{I} \dots$$

This equation is now exactly in the form in which the recursion method [33] may be applied. At this point we note that the above expression for the averaged $G_{LL}(\mathbf{k}, z)$ is exact.

The recursion method addresses inversions of infinite matrices. Once a sparse representation of an operator in

Hilbert space, $\tilde{\mathbf{H}}^{(2)}$, is known in a countable basis, the recursion method obtains an alternative basis in which the operator becomes tridiagonal. This basis and the representations of the operator in it are found recursively through a three-term recurrence relation :

$$|u_{n+1}\rangle = \tilde{\mathbf{H}}^{(2)}|u_n\rangle - \alpha_n(\mathbf{k})|u_n\rangle - \beta_n^2(\mathbf{k})|u_{n-1}\rangle. \quad (9)$$

with the initial choice $|u_1\rangle = |\mathbf{k}L\rangle \otimes |\{\emptyset\}\rangle$ and $\beta_1^2 = 1$. The recursion coefficients α_n and β_n are obtained by imposing the ortho-normalizability condition of the new basis set as :

$$\alpha_n(\mathbf{k}) = \frac{\{n|\tilde{\mathbf{H}}^{(2)}|n\}}{\{n|n\}} ; \quad \beta_{n-1}^2(\mathbf{k}) = \frac{\{n-1|\tilde{\mathbf{H}}^{(2)}|n\}}{\{n|n\}}$$

and also $\{m|\tilde{\mathbf{H}}^{(2)}|n\} = 0$ for $m \neq n, n \pm 1$

To obtain the spectral function we first write the configuration averaged L -projected Green functions as continued fractions :

$$\ll G_{LL}(\mathbf{k}, z) \gg = \frac{\beta_{1L}^2}{z - \alpha_{1L}(\mathbf{k}) - \frac{\beta_{2L}^2(\mathbf{k})}{z - \alpha_{2L}(\mathbf{k}) - \frac{\beta_{3L}^2(\mathbf{k})}{\ddots - \frac{\beta_{NL}^2(\mathbf{k}) - \mathbf{\Gamma}_L(\mathbf{k}, z)}{}}}}.$$

where $\mathbf{\Gamma}_L(\mathbf{k}, z)$ is the asymptotic part of the continued fraction. The approximation involved has to do with the termination of this continued fraction. The coefficients are calculated exactly up to a finite number of steps $\{\alpha_n, \beta_n\}$ for $n < N$ and the asymptotic part of the continued fraction is obtained from the initial set of coefficients using the idea of Beer and Pettifor terminator [34]. Haydock and coworkers [35] have carried out extensive studies of the errors involved and precise estimates are available in the literature. Haydock [36] has shown that if we carry out recursion exactly up to N steps, the resulting continued fraction maintains the first $2N$ moments of the exact result.

It is important to note that the operators $\tilde{\mathbf{A}}, \tilde{\mathbf{B}}, \tilde{\mathbf{F}}$ are

all projection operators in real space (i.e unit operators in \mathbf{k} -space) and acts on an augmented space basis only to change the configuration part (i.e. the cardinality sequence $\{\mathcal{C}\}$).

$$\begin{aligned} \tilde{\mathbf{A}}|\{\mathcal{C}\}\rangle &= A_1|\{\mathcal{C}\}\rangle, \\ \tilde{\mathbf{B}}|\{\mathcal{C}\}\rangle &= A_2|\{\mathcal{C}\}\rangle \delta(R \in \{\mathcal{C}\}), \\ \tilde{\mathbf{F}}|\{\mathcal{C}\}\rangle &= A_3|\{\mathcal{C} \pm R\}\rangle. \end{aligned}$$

The coefficients $A_1 - A_3$ can be expressed from equation (8). The remaining operator $\tilde{\mathbf{S}}$ is diagonal in \mathbf{k} -space and acts on an augmented space only to change

the configuration part :

$$\tilde{\mathbf{S}}||\{\mathcal{C}\}\rangle = \sum_{\chi} \exp(-i\mathbf{k}\cdot\chi) ||\{\mathcal{C} - \chi\}\rangle.$$

Here χ s are the near neighbour vectors. The operation of the effective Hamiltonian is thus entirely in the configuration space and the calculation does not involve the space \mathcal{H} at all. This is an enormous simplification over the standard augmented space recursion [24, 28, 29, 30], where the entire reduced real space part as well as the configuration part were involved in the recursion process. Earlier we had to resort to symmetry reduction of this enormous space in order to make the recursion tractable. Here the rank of only the configuration space is much smaller and we may further reduce it by using the local symmetries of the configuration space, as described in our earlier letter [24]. However, this advantage is offset by the fact that the effective Hamiltonian is energy dependent. This means that to obtain the Green functions we have to carry out the recursion for each energy point. This process is simplified by carrying out recursion over a suitably chosen set of *seed energies* and interpolating the values of the coefficients across the band.

The self-energy which arises because of scattering by the random potential fluctuations is of the form :

$$\Sigma_L(\mathbf{k}, z) = \frac{\beta_{2L}^2(\mathbf{k})}{z - \alpha_{2L}(\mathbf{k}) - \frac{\beta_{3L}^2(\mathbf{k})}{\ddots - \frac{\ddots}{z - \alpha_{NL}(\mathbf{k}) - \Gamma_L(\mathbf{k}, z)}}}.$$

So the continued fraction can be written in the form $1/(z - \tilde{E}_L(\mathbf{k}) - \Sigma_L(\mathbf{k}, E))$, where $\tilde{E}_L(\mathbf{k}) = \alpha_{1L}(\mathbf{k})$.

The average spectral function $\ll A_{\mathbf{k}}(E) \gg$ is related to the averaged Green function in reciprocal space as :

$$\ll A_{\mathbf{k}}(E) \gg = \sum_L \ll A_{\mathbf{k}L}(E) \gg,$$

where

$$\ll A_{\mathbf{k}L}(E) \gg = -\frac{1}{\pi} \lim_{\delta \rightarrow 0+} \{\text{Im} \ll G_{LL}(\mathbf{k}, E - i\delta) \gg\}.$$

To obtain the complex bands for the alloy we fix a value for \mathbf{k} and solve for :

$$z - \tilde{E}_L(\mathbf{k}) - \Sigma_L(\mathbf{k}, E) = 0.$$

The real part of the roots will give the position of the bands, while the imaginary part of roots will be proportional to the lifetime. Since the alloy is random, the bands always have finite lifetimes and are fuzzy.

We have used this reciprocal space ASR to obtain the complex bands and spectral functions for the CuZn alloy. This is shown in Figs. (2) - (3). It should be noted that we have carried out a fully LDA self-consistent calculation using the TB-LMTO-ASR developed by us [37] to obtain the potential parameters. It takes care of the charge transfer effects. For the Madelung energy part of the alloy calculation, we have chosen the approach of Ruban and Skriver [38].

The two panels of Fig. (2) compare the band structures of pure Cu and pure Zn metals in the same bcc lattice as the 50-50 alloy. We note that the *s*-like bands of Cu and Zn stretch from -0.8 Ry., while the *d*-like states of Zn and Cu, whose degeneracies are lifted by the cubic symmetry of the bcc lattice are more localized and reside in the neighbourhood of -0.6 Ry. and between -0.3 to -0.2 Ry. respectively. The complex bands of the solid clearly reflect the same band structure. However, the bands are slightly shifted and broadened because of the disorder scattering of Bloch states in the disordered alloy. The scattering lifetimes are maximum for the Cu *d*-like bands, less for the Zn *d*-like bands and minimum for the lower *s*-like bands. This is expected, since the delocalized *s*-like states straddle large volumes of the lattice space and are therefore less sensitive to the local configuration fluctuations of the substitutional alloy.

The same is reflected in the spectral functions, shown here also along the Γ - X direction in the Brillouin zone. Sharp peaks stretching from -0.8 Ry., groups of wider peaks around -0.6 Ry. with less dispersion, characteristic of the more localized *d*-like states and groups of much wider peaks straddling -0.3–0.2 Ry. also with less dispersion. The spectral functions play an important role in response functions related to photoemission and optical conductivity [58]. Our complex bands agree remarkably well with the Fig.3 of Bansil and Ehrenreich [4]. These authors of course did not show the dispersion of the Zn *d*-bands, but as in their work, the Cu bands show greater disorder induced lifetimes than the lower energy Zn *d*-bands.

We may use the generalized tetrahedron method to pass from the reciprocal space spectral functions to the real space density of states [59]. Alternatively, we may also carry out real-space ASR to obtain the density of states directly.

Fig. (4) shows the densities of states for the pure Zn (solid lines) and Cu (dashed lines) in the same bcc lattice as the alloy and compares this with the ordered B2 and disordered bcc 50-50 CuZn alloy. We first note that in the ordered B2 alloy there is a considerable narrowing of the Zn well as the Cu *d*-like bands. The feature around -0.3 Ry. is suppressed in the ordered alloy. In the disordered alloy on the other hand, although disorder scattering introduces life-time effects which washes out the sharp structures in the ordered systems, the re-

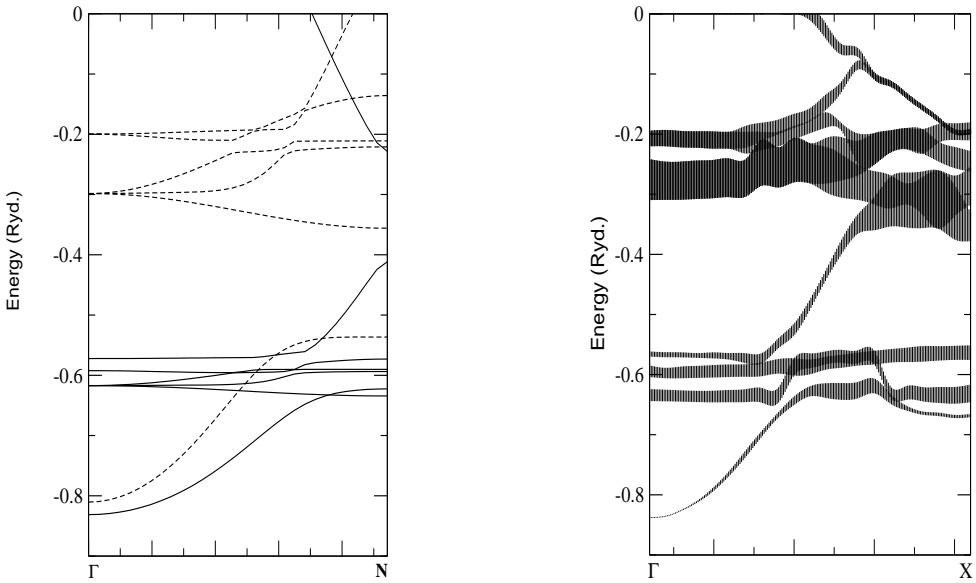


FIG. 2: (left) Bands for pure Cu and Zn in bcc lattices with the same lattice parameter as the 50-50 CuZn alloy. The dashed line are for Cu and the full lines for Zn. (right) Complex bands for the 50-50 CuZn alloy.

semblance to the pure metals is evident. As seen in the complex bands, the life-time effects in the Cu d -like part is prominent. If we interpret the left most figure as that due to completely segregated Cu-Zn and the middle one as the completely ordered one, then the disordered alloy lies between the two. In the next section, introducing short-ranged ordering effects on top of the fully disordered alloy, we shall study how to bridge between the two states.

SHORT-RANGED ORDERING IN THE ALLOYS

Attempts at developing generalizations of the coherent potential approximation (CPA) to include effects of short-ranged order (SRO) have been many, spread over the last several decades. The CPA being a single site mean-field approximation cannot take into account SRO as it spans at least a nearest neighbour cluster on the lattice. The early attempts at cluster-generalizations of the CPA were beset with difficulties of violation of the analytic properties of the approximated configuration averaged Green function. Tsukada's [39] idea of introducing a super-cell the size of the cluster in an effective medium suffered from the problem of broken translational symmetry within the cluster even when the disorder was homogeneous. This same problem beset the CCPA's proposed by Kumar *et.al.* [40] based on the augmented space theorem introduced by Mookerjee [26]. The embedded cluster method of Gonis *et.al.* [42] immersed a cluster in a CPA medium which lacked the full self-consistency with it. The first, translationally symmetric cluster approximations which preserved the analytic properties of the approximate Green functions were all based on the augmented space theorem of Mookerjee [26]. They included the travelling cluster approximation (TCA) of Kaplan and Gray [27] and Mills and Ratnavaraka [44] and the CCPA proposed by Razee *et.al.* [45]. The problem with these approaches was that they became intractable as the size of the cluster considered was increased much beyond two sites. Mookerjee and Prasad [46] generalized the augmented space theorem to include correlated disorder. However, since they then went on to apply it in the CCPA approximation, they could not go beyond the

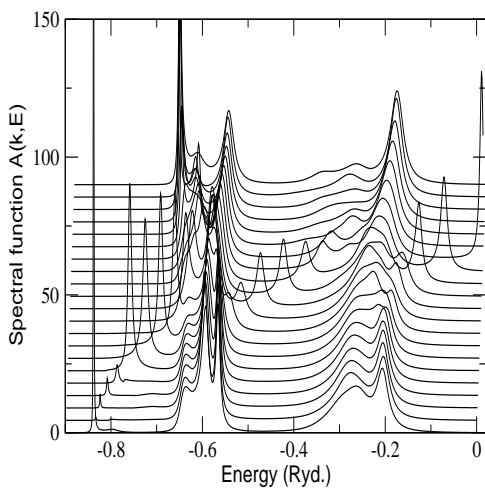


FIG. 3: Spectral functions for the CuZn alloy for \mathbf{k} -vectors along the Γ to X direction in the Brillouin zone.

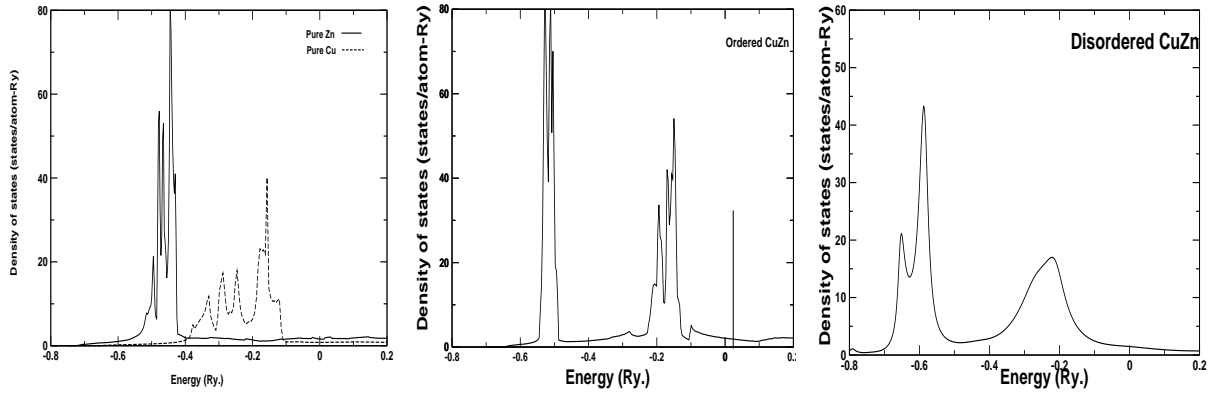


FIG. 4: (left) Density of states of pure Zn (solid lines) and Cu (dashed lines) in the same bcc lattice as the 50-50 CuZn alloy. (centre) Density of states for ordered B2 50-50 CuZn alloy. (right) Density of states for the disordered bcc 50-50 CuZn alloy.

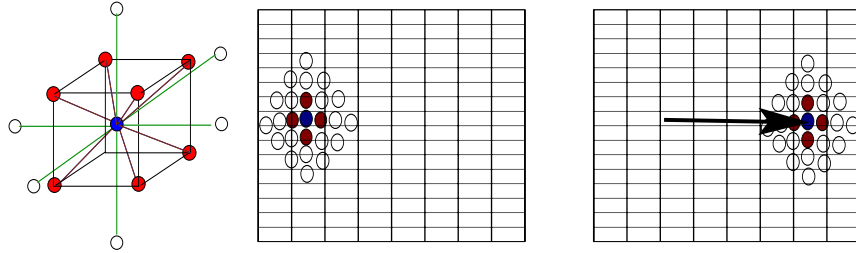


FIG. 5: (Color Online) (left) The blue atom represents the site labelled 0, where the local density of states will be calculated. The red atoms are its eight nearest neighbours on the bcc lattice. The white atoms are more distant neighbours (right) Schematic diagram showing lattice translational symmetry of the nearest neighbour cluster SRO approach.

two-site cluster and that too to model systems alone. The breakthrough came with the augmented space recursion (ASR) approach proposed by Saha et.al. [47]-[48]. The method was a departure from the mean-field approaches which always began by embedding a cluster in an effective medium which was then obtained self-consistently. Here the Green function was expanded in a continued fraction whose asymptotic part was obtained from its initial steps through an ingenious *termination* procedure [33]. In this method the effect at a site of quite a large environment around it could be taken into account depending how far one went down the continued fraction before *termination*. The technique was made fully LDA-self-consistent within the tight-binding linear muffin-tin orbitals (TB-LMTO) approach [49] and several applications have been carried out to include short-ranged order in different alloy systems [50]. Recently Leath and co-workers have developed an itinerant CPA (ICPA) based on the augmented space theorem [51], which also maintains both analyticity and translational symmetry and takes into account effect of the nearest neighbour environment of a site in an alloy. The technique has been very successfully applied to the phonon problem in alloys where there were large force constant disorders. This method matches well with the ASR approach to the same alloys [52] and there is now a concerted effort to apply it to electronic problems based

on both the TB-KKR and the TB-LMTO methods. A very different and rather striking approach has been developed by Rowlands et.al. [53] (the non-local CPA or NL-CPA) using the idea of *coarse graining* in reciprocal space originally proposed by Jarell and Krishnamurthy [6]. The NL-CPA with SRO has been applied earlier by Rowlands et.al. [5] and is on the verge of being made fully DFT self-consistent within the KKR. The authors report an unpublished report on it [54]. In this communication we report a fully DFT self-consistent ASR based on the TB-LMTO with SRO incorporated. We have applied it to the case of 50-50 CuZn alloys, so as to have a comparison with earlier attempts using different techniques.

THE GENERALIZED AUGMENTED SPACE THEOREM

The generalized augmented space theorem has been described in detail by Mookerjee and Prasad [46]. Let us briefly introduce those essential ideas which are necessary to make this communication reasonably self-contained.

For a substitutionally binary disordered alloy A_xB_y on a lattice we can introduce a set of random occupation variables $\{n_R\}$ associated with the lattice sites labelled by R , which take the values 0 or 1 depending upon whether

the site R is occupied by a A or a B type of atom. The Hamiltonian and hence the Green function are both functions of this set of random variables. The configuration averaged Green operator is then :

$$\ll G(z, \{n_R\}) \gg = \int \dots \int \prod_R dn_R G(z, \{n_R\}) P(\{n_R\})$$

To start with, let us assume that short-ranged order extends up to nearest neighbours only. Let us take for an example the nearest neighbour cluster of nine atoms on a body centered cubic lattice (see Fig. 5) centered on the site labelled by $i = 0$. Let us concentrate on the central atom (labelled 0). The occupation variables associated with its eight neighbours are correlated with n_1 , but not with one another. Further none of the other occupation variables associated with more distant sites are correlated with n_1 . If we label any other site k as 0, that is carry out a lattice translation from the site i to k , its environment is identical to the earlier situation. Therefore the subsequent procedure is translationally symmetric, as it should be, if the SRO is itself homogeneous. We may then write :

$$P(n_0, n_2, \dots, n_k, \dots) = P(n_0) \prod_{j=1}^8 P(n_j|n_1) \prod_{k>8} P(n_k)$$

The generalized Augmented Space Theorem then associates with the random variables $\{n_k\}$ corresponding operators $\{\widetilde{\mathbf{M}}_k\}$ in their configuration space. The construction of the representations of these operators has been discussed in detail in the paper by Mookerjee and Prasad [46]. Here we shall quote only the relevant results necessary to proceed further.

We shall characterize the SRO by a Warren-Cowley parameter α . In terms of this the probability densities are given by : for $k=0$ and $k>8$.

$$P(n_k) = x\delta(n_k - 1) + y\delta(n_k), \quad x + y = 1$$

While for $j=1,2,\dots,8$:

$$\begin{aligned} P(n_j|n_0 = 1) &= (x + \alpha y)\delta(n_j - 1) + (1 - \alpha)y\delta(n_j) \\ P(n_j|n_0 = 0) &= (1 - \alpha)x\delta(n_j - 1) + (y + \alpha x)\delta(n_j) \end{aligned} \quad (10)$$

In terms of the concentrations x and y and SRO parameter α these operators have representations :

$$\begin{aligned} \mathbf{M}_k &= \begin{pmatrix} x & \sqrt{xy} \\ \sqrt{xy} & y \end{pmatrix}, \quad k = 0, \text{ or } k > 8 \\ \mathbf{M}_j^1 &= \begin{pmatrix} x + \alpha y & \sqrt{(1 - \alpha)y(x + \alpha y)} \\ \sqrt{(1 - \alpha)y(x + \alpha y)} & (1 - \alpha)y \end{pmatrix}, \\ \mathbf{M}_j^0 &= \begin{pmatrix} (1 - \alpha)x & \sqrt{(1 - \alpha)x(y + \alpha x)} \\ \sqrt{(1 - \alpha)x(y + \alpha x)} & y + \alpha x \end{pmatrix}, \\ j &= 1, 2, \dots, 8 \end{aligned} \quad (11)$$

The projection operators at the site labelled 0 are :

$$\begin{aligned} \mathbf{P}_0^1 &= \begin{pmatrix} x & \sqrt{xy} \\ \sqrt{xy} & y \end{pmatrix}, \\ \mathbf{P}_0^0 &= \begin{pmatrix} y & -\sqrt{xy} \\ -\sqrt{xy} & x \end{pmatrix}, \end{aligned} \quad (12)$$

In the full augmented space, which is the product space of all the individual configuration space of the different occupation variables, the operators which replace the occupation variables are :

$$\begin{aligned} \widetilde{\mathbf{M}}_0 &= M_1 \otimes I \otimes I \otimes \dots \\ \widetilde{\mathbf{M}}_j &= \sum_{k=0}^1 P_1^k \otimes M_2^k \otimes I \otimes \dots \quad j=1, 2, \dots, 8 \\ \widetilde{\mathbf{M}}_k &= I \otimes I \otimes \dots M_k \otimes I \otimes \dots \quad k > 8 \end{aligned} \quad (13)$$

In operator form the operators labelled by 0 and $k > 8$ have the same form as in Equation (4). The operators labelled by j have the form :

$$\begin{aligned} \widetilde{\mathbf{M}}_j &= x \mathcal{I} \otimes \mathcal{I} \dots + b(x) \mathcal{P}_j^\downarrow \otimes \mathcal{I} \dots + b'(x) \mathcal{P}_0^\downarrow \otimes \mathcal{I} \dots + f''(x) \mathcal{T}_0^{\uparrow\downarrow} \otimes \mathcal{I} \dots + b''(x) \mathcal{P}_0^\downarrow \otimes \mathcal{P}_j^\downarrow \otimes \dots \\ &\quad + f'(x) \mathcal{T}_j^{\uparrow\downarrow} \otimes \mathcal{I} \dots + d''(x) \mathcal{P}_0^\downarrow \otimes \mathcal{T}_j^{\uparrow\downarrow} \dots + d(x) \mathcal{T}_0^{\uparrow\downarrow} \otimes \mathcal{P}_j^\downarrow \dots + f'''(x) \mathcal{T}_0^{\uparrow\downarrow} \otimes \mathcal{T}_j^{\uparrow\downarrow} \dots \end{aligned} \quad (14)$$

where,

$$\begin{aligned} b'(x) &= \alpha(y - x) & b''(x) &= -2\alpha(y - x) & F'(x) &= (x\beta_1 + y\beta_2) & F''(x) &= \alpha\sqrt{xy} \\ F'''(x) &= (\beta_1 - \beta_2)\sqrt{xy}; & D(x) &= -2\alpha\sqrt{xy}; & D''(x) &= (y - x)(\beta_1 - \beta_2) \\ \beta_1 &= \sqrt{(1 - \alpha)y(x + \alpha y)}; & \beta_2 &= \sqrt{(1 - \alpha)x(y + \alpha x)} \end{aligned}$$

We now follow the augmented space theorem and replace all the occupation variables $\{n_R\}$ by their corresponding operators.

It is easy to check that in the absence of short-ranged order the functions $b'(x)$, $b''(x)$, $f''(x)$, $f'''(x)$, $d(x)$ and $d'(x)$ all vanish, $\beta_1 = \beta_2 = \sqrt{xy}$ and $f'(x) = f(x)$. We also note that the choice of the central site labelled '0' is immaterial. If we translate this site to any other and apply the lattice translation to all the sites, hence the Hamiltonian in the full augmented space, remains unchanged. This formulation of short ranged order also possesses lattice translational symmetry, provided the short-ranged order is homogeneous in space.

EFFECT OF SRO ON THE DENSITY OF STATES

We have carried out the TB-LMTO-ASR calculations on CuZn with a lattice constant of 2.85 Å. The Cu and Zn potentials are self-consistently obtained via the LDA self-consistency loop. All reciprocal space integrals are done by using the generalized tetrahedron integration for disordered systems introduced by us earlier [59].

To discuss the effect of SRO, leading, on one hand, to ordering ($\alpha < 0$) and segregation on the other ($\alpha > 0$), let us first look at Figs. 2 and 4. The complex band structure shown in Fig. 2 shows that the system is a *split band* alloy. The positions of the *d*-bands of Cu and Zn are well separated in energy. This implies that the "electrons travel more easily between Cu or between Zn sites than between unlike ones" [5]. So when the alloy orders and unlike sites sit next to each other, the overlap integral between the like sites decrease. This leads to a narrowing of the bands associated with Cu and Zn. A comparison between the leftmost and central panels of Fig. 4 shows that the bandwidths in the latter are almost half of the former. This should be the main effect of ordering setting in. On the other hand, when the alloy is completely disordered, the bands gets widened by disorder scattering and the sharp structures in the density of states are smoothed.

Fig. (6) shows the density of states with increasing positive α . Positive α indicates a clustering tendency. Comparing with Fig. (4) we note that as clustering tendency increases the density of states begins to show the structures seen in the pure metals in both the split bands. For large positive α there is still residual long-ranged disorder. This causes smoothing of the bands with respect to the pure materials. For these large, positive α s, we notice the development of the structure around -0.3 Ry.

Fig. (7) shows the density of states with increasing negative α which indicates increasing ordering tendency. On the bcc lattice at 50-50 composition we expect this ordering to favour a B2 structure. With increasing ordering

tendency, both the split bands narrow and lose structure. The feature around -0.3 Ry. disappears. This band narrowing and suppression of the feature around -0.3 Ry. is clearly seen in the ordered B2 alloy shown in Fig. (4).

Our analysis is closely similar to that of Rowlands *et.al.* [5]. However, there are quantitative differences as both the basic technique (KKR and TB-LMTO) and the approximations are quantitatively different. Finally, in Fig. 8 we show the band energy as a function of the nearest neighbour Warren-Cowley parameter. The minimum occurs at the ordering end, as expected. Experimentally the alloy does show a tendency to order at lower temperatures.

OPTICAL PROPERTIES OF CUZN ALLOYS

In an earlier work [55] we had developed a methodology for the calculation of configuration averaged optical conductivity of a disordered alloy based on the augmented space formalism. Here we shall present the salient features required for the calculation of optical response functions in the 50-50 CuZn alloy.

In linear response theory, at zero temperature, the generalized susceptibility of a disordered alloy is given by the Kubo formula :

$$\langle \mathbf{j}^\mu(t) \rangle = \int_{-\infty}^{\infty} \chi^{\mu\nu}(t-t') A^\nu(t')$$

where, $A^\nu(t)$ is the vector potential, and

$$\chi^{\mu\nu}(t-t') = (i/\hbar) \Theta(t-t') \langle [\mathbf{j}^\mu(t) \mathbf{j}^\nu(t')] \rangle$$

\mathbf{j}^μ is the current operator and Θ is the Heaviside step function. If the underlying lattice has cubic symmetry, $\chi^{\mu\nu} = \chi \delta_{\mu\nu}$. The fluctuation dissipation theorem then relates the imaginary part of the Laplace transform of the generalized susceptibility to the Laplace transform of a correlation function :

$$\chi''(\omega) = (1/2\hbar) (1 - \exp\{-\beta\hbar\omega\}) S(\omega)$$

where,

$$S(\omega) = \int_0^{\infty} dt \exp\{i(\omega + i\delta)t\} \text{Tr} \left(\mathbf{j}^\mu(t) \mathbf{j}^\mu(0) \right) \quad (15)$$

Since the response function is independent of the direction label μ for cubic symmetry, in the following we shall drop this symbol. In case of other symmetries we have to generalize our results for different directions. Our goal

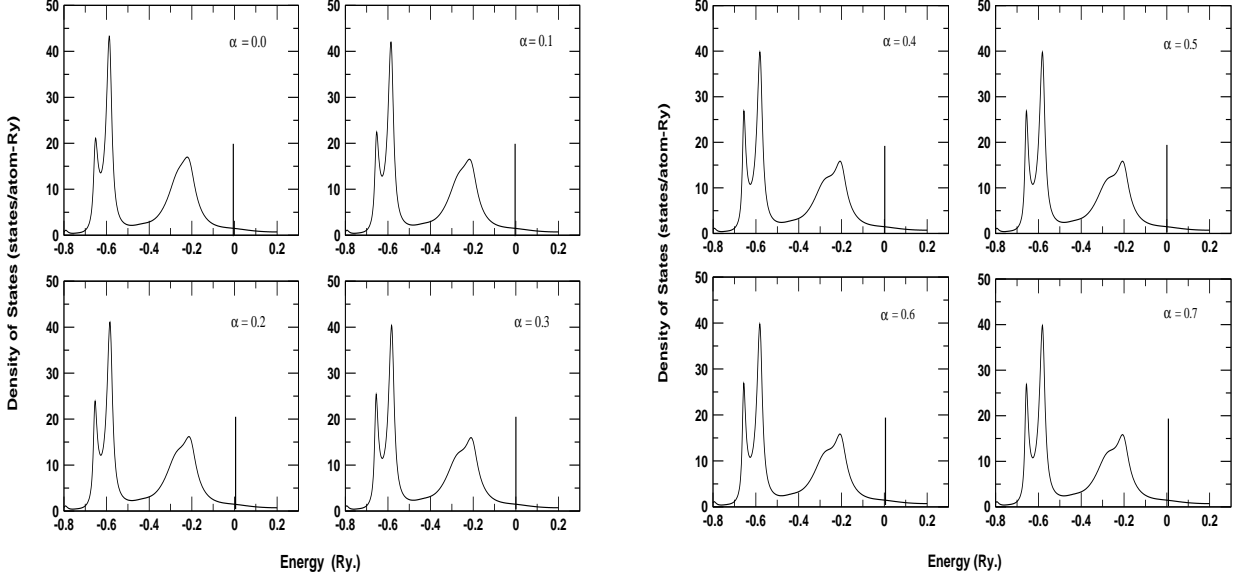


FIG. 6: Density of states for 50-50 CuZn with increasing positive α which describes increasing clustering tendency

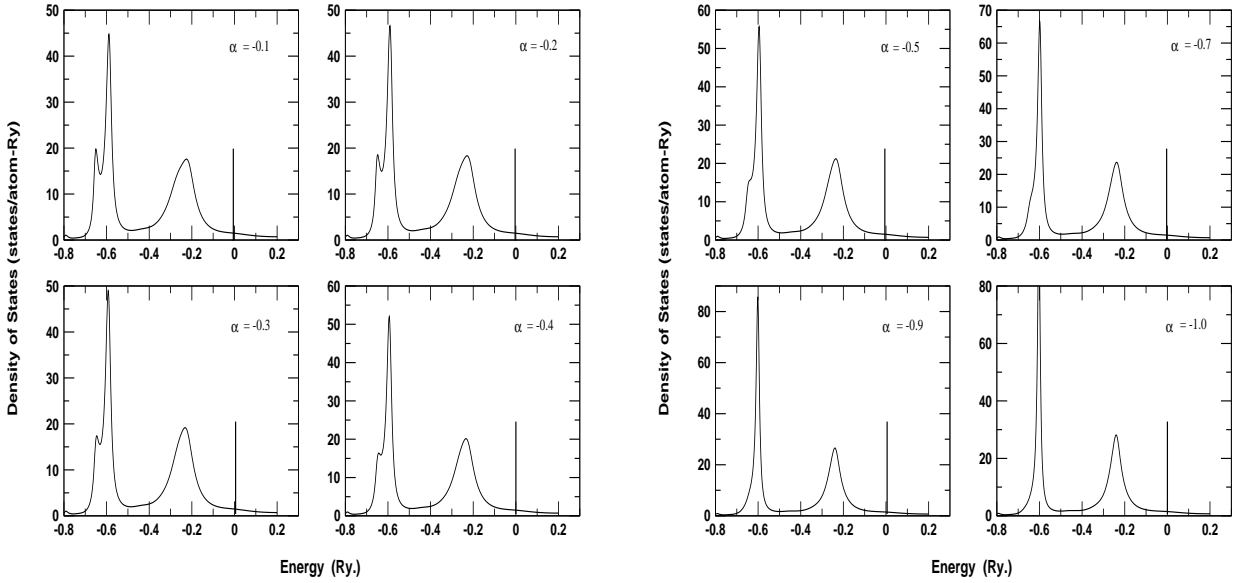


FIG. 7: Density of states for 50-50 CuZn with increasing negative α which describes increasing ordering tendency

will be, given a quantum “Hamiltonian” \mathbf{H} to obtain the correlation function : $S(t) = \langle \phi | \mathbf{j}(t) \mathbf{j}(0) | \phi \rangle$

We shall now determine the correlation directly via the recursion method as described by Viswanath and Müller[56].

For a disordered binary alloy, $S(t) = S[\bar{\mathbf{H}}(\{n_R\})]$. The

augmented space theorem then states that :

$$\ll S(t) \gg = \ll \langle \phi | \mathbf{j}(t) \mathbf{j}(0) | \phi \rangle \gg \\ = \langle \phi \otimes \{\emptyset\} | \tilde{\mathbf{j}}(t) \tilde{\mathbf{j}}(0) | \phi \otimes \{\emptyset\} \rangle = S[\tilde{\mathbf{H}}(\{\tilde{\mathbf{M}}^R\})]$$

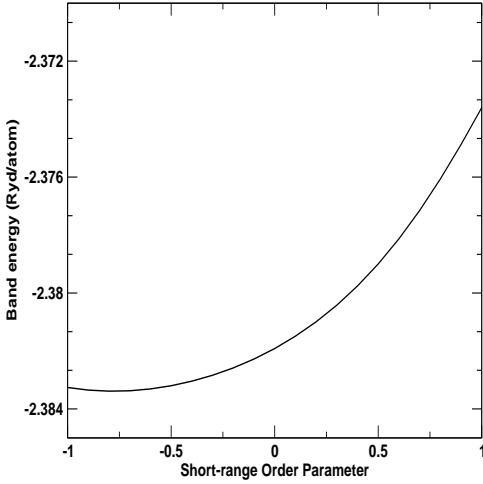


FIG. 8: The Band energy (from which the contribution of the core electrons have been subtracted) as a function of the nearest-neighbour Warren-Cowley SRO parameter

where the augmented space Hamiltonian and the current operators are constructed by replacing every random variable n_R by the corresponding operator $\tilde{\mathbf{M}}^R$.

The recursion may now be modified step by step in the full augmented space :

$$\langle \psi(t) | = \langle \phi \otimes \{\emptyset\} | \tilde{\mathbf{j}}(t)$$

The time evolution of this bra is governed by the Schrödinger equation

$$-i \frac{d}{dt} \left\{ \langle \psi(t) | \right\} = \langle \psi(t) | \tilde{\mathbf{H}} \quad (16)$$

As before, we shall generate the orthogonal basis $\{ \langle f_k | \}$ for representation of equation (16) :

(i) We begin with initial conditions :

$$\langle f_{-1} | = 0 \quad ; \quad \langle f_0 | = \langle \phi \otimes \{\emptyset\} | \tilde{\mathbf{j}}(0)$$

(ii) The new basis members are generated by a three term recurrence relationship :

$$\langle f_{k+1} | = \langle f_k | \tilde{\mathbf{H}} - \langle f_k | \tilde{\alpha}_k - \langle f_{k-1} | \tilde{\beta}_k^2 \quad k = 0, 1, 2 \dots$$

where,

$$\tilde{\alpha}_k = \frac{\langle f_k | \tilde{\mathbf{H}} | f_k \rangle}{\langle f_k | f_k \rangle} \quad \tilde{\beta}_k^2 = \frac{\langle f_k | f_k \rangle}{\langle f_{k-1} | f_{k-1} \rangle} \quad (17)$$

We now expand the bra $\langle \psi(t) |$ in this orthogonal basis :

$$\langle \psi(t) \otimes \{\emptyset\} | = \sum_{k=0}^{\infty} \langle f_k | \tilde{D}_k(t)$$

Continuing exactly as in the last section we get,

$$\tilde{D}_0(t) = \langle \psi(t) \otimes \{\emptyset\} | f_0 \rangle = \ll S(t) \gg \quad (18)$$

Taking Laplace transforms and using the three term recurrence,

$$\tilde{d}_0(z) = \frac{i}{z - \tilde{\alpha}_0 - \frac{\tilde{\beta}_1^2}{z - \tilde{\alpha}_1 - \frac{\tilde{\beta}_2^2}{z - \tilde{\alpha}_2 - \dots}}} \quad (19)$$

The configuration averaged structure function, which is the Laplace transform of the averaged correlation function can then be obtained from the above :

$$\ll S(\omega) \gg = \lim_{\delta \rightarrow 0} 2 \operatorname{Re} \tilde{d}_0(\omega + i\delta) \quad (20)$$

The imaginary part of the dielectric function is related to this correlation function through :

$$\epsilon_2(\omega) = \frac{\ll S(\omega) \gg}{\omega}$$

The real part of the dielectric function is related to the imaginary part through a Kramers-Krönig relationship. The equations (17)-(20) will form the basis of our calculation of the configuration averaged correlation function.

Next we look at the expression for the current operator in the TB-LMTO basis :

$$|\chi_R \rangle = |\phi_R \rangle + \sum_{R'} h_{RR'} |\dot{\phi}_{R'} \rangle$$

The dot refers to derivative with respect to energy. In this basis, the matrix elements of the current operator can be written as

$$J_{RR'}^\mu = \langle \chi_{R'} | \mathbf{j}^\mu | \chi_R \rangle$$

where,

$$J_{RR'}^\mu = e \left[V_{RR'}^{(1),\mu} \delta_{RR'} + \sum_{R''} V_{RR''}^{(2),\mu} h_{R''R'} + \dots \right. \\ \left. \sum_{R''} h_{RR''} V_{R''R'}^{(3),\mu} + \sum_{R''} \sum_{R'''} h_{RR'''} V_{R'''R'}^{(4),\mu} h_{R''R'} \right] \quad (21)$$

with,

$$\begin{aligned} V_{RR'}^{(1),\mu} &= \langle \phi_{R'} | \mathbf{v}^\mu | \phi_R \rangle ; \quad V_{RR'}^{(2),\mu} = \langle \dot{\phi}_{R'} | \mathbf{v}^\mu | \phi_R \rangle \\ V_{RR'}^{(3),\mu} &= \langle \phi_{R'} | \mathbf{v}^\mu | \dot{\phi}_R \rangle ; \quad V_{RR'}^{(4),\mu} = \langle \dot{\phi}_{R'} | \mathbf{v}^\mu | \dot{\phi}_R \rangle \end{aligned}$$

The technique for calculating these matrix elements has been described in detailed by Hobbs *et.al.* [57]. We have also used this technique in our earlier paper [58] and we shall use it here as well. The readers are referred to these two papers for details.

Ideally the next step would be to calculate $J_{AA}^\mu, J_{BB}^\mu, J_{AB}^\mu, J_{BA}^\mu$ as the current terms between two sites when they are occupied by atom pairs AA, BB, AB and BA embedded in the disordered medium. A simpler first step would be to obtain these current terms from the pure A and B and from the ordered AB alloy. In general, the current operator can be written as :

$$\mathbf{j}^\mu = \sum_R J^\mu(0) \mathbf{P}_R + \sum_R \sum_{R'} J^\mu(\chi) \mathbf{T}_{RR'} \quad (22)$$

where $\chi = R - R'$.

In a disordered alloy, the representations of the current operators are random :

$$\begin{aligned} J^\mu(0) &= J_{AA}^\mu(0) n_R + J_{BB}^\mu(0) (1 - n_R) \quad \text{and} \\ J^\mu(\chi) &= J_{AA}^\mu(\chi) n_R n_{R'} + J_{BB}^\mu(\chi) (1 - n_R) (1 - n_{R'}) + \\ &\quad J_{AB}^\mu(\chi) n_R (1 - n_{R'}) + J_{BA}^\mu(\chi) (1 - n_R) n_{R'} \end{aligned}$$

Where $R - R' = \chi$. Using the augmented space theorem, we replace the random variable n_R by an operator M^R in the expressions for $J^\mu(0)$ and $J^\mu(\chi)$ we get the current operator in the augmented space :

$$\begin{aligned} \tilde{\mathbf{j}}^\mu = \sum_R \left\{ J_{BB}^\mu(0) \mathcal{P}_R \otimes \tilde{\mathbf{I}} \dots + J_1^\mu(0) \mathcal{P}_R \otimes \widetilde{\mathbf{M}}_R \right\} + \sum_R \sum_{R'} \left\{ J_{BB}^\mu(\chi) \mathcal{T}_{RR'} \otimes \tilde{\mathbf{I}} + J_1^\mu(\chi) \mathcal{T}_{RR'} \otimes \left(\widetilde{\mathbf{M}}_R + \widetilde{\mathbf{M}}_{R'} \right) + \right. \\ \left. J_2^\mu(\chi) \mathcal{T}_{RR'} \otimes \widetilde{\mathbf{M}}_R \otimes \widetilde{\mathbf{M}}_{R'} \right\} \end{aligned} \quad (23)$$

$$\begin{aligned} J_1^\mu(0) &= [J_{AA}^\mu(0) - J_{BB}^\mu(0)]; & J_2^\mu(0) &= [J_{AA}^\mu(0) - J_{BB}^\mu(0)] \\ J_1^\mu(\chi) &= [J_{AA}^\mu(\chi) - J_{BB}^\mu(\chi)]; & J_2^\mu(\chi) &= [J_{AA}^\mu(\chi) - J_{BB}^\mu(\chi)] \\ J_3^\mu(\chi) &= J_{AA}^\mu(\chi) - J_{AB}^\mu(\chi) - J_{BA}^\mu(\chi) + J_{BB}^\mu(\chi) \end{aligned}$$

The relevant operators are now chosen from Equations (4) and (14) and the current operator in full augmented space is set up from them. This augmented current operator is used to construct the starting state of the recursion as described in the last section.

Since the real part of the dielectric function $\epsilon_1(\omega)$ can be now obtained from the imaginary part $\epsilon_2(\omega)$ using a Kramers Krönig relationship, we know the full complex dielectric function. All optical response functions may now be derived from these. If we assume the orientation of the crystal surface to be parallel to the optic axis, the reflectivity $R(\omega)$ follows directly from Fresnel's formula :

$$R(\omega) = \left| \frac{\sqrt{\epsilon(\omega)} - 1}{\sqrt{\epsilon(\omega)} + 1} \right|^2$$

Fig. 9 (top panel) shows the imaginary part of the dielectric function varying with frequency showing increasing

segregating tendency. If we examine the density of states for both the ordered and disordered alloys we note that it is only around or just above $\hbar\omega \simeq 0.1$ Ry that the transitions from the d -bands of Cu begin to contribute to $\epsilon_2(\omega)$. Below this energy, the behaviour is Drude like. This is clearly seen in the panels of the figure. As α increases and the alloy tends to segregate, since the weight of the structure in the density of states nearer to the Fermi-energy, increases, this contribution leads to the increasing weight of the structure near 0.1 Ry.

Fig. 9 (bottom panel) shows the variation of $\epsilon_2(\omega)$ with the nearest neighbour Warren-Cowley SRO parameter showing increased ordering tendency. The narrowing of the band with ordering and the increase of weightage to the structure away from the Fermi energy is clearly reflected in the dielectric function. It is also obvious from the figures that the imaginary part of the dielectric function is more sensitive to the variation of short-ranged order than the density of states.

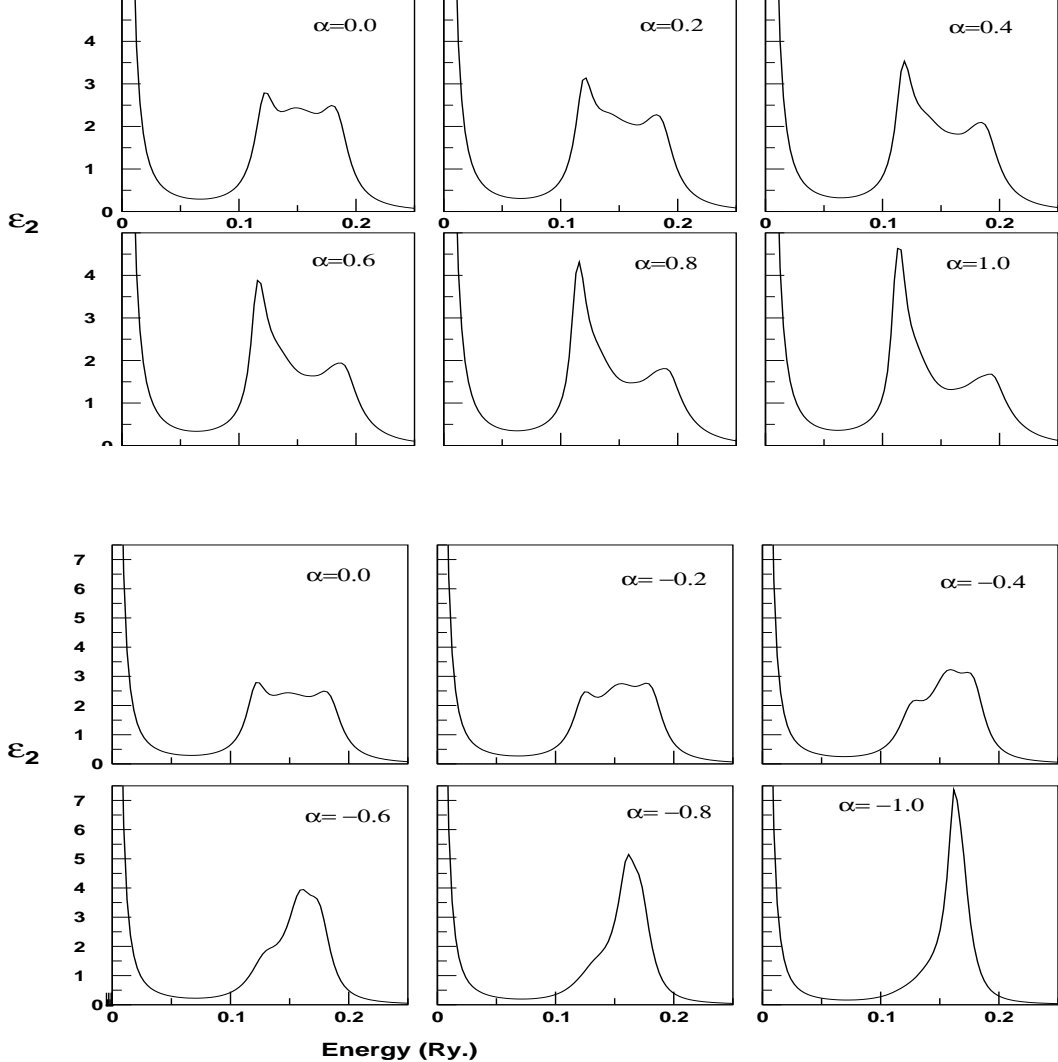


FIG. 9: (Top panel)Imaginary part of the dielectric function as a function of energy and its variation with the nearest neighbour Warren-Cowley SRO parameter, $\alpha > 0$ increasing, indicating segregating tendency. (Bottom panel) The same with $\alpha < 0$ increasing, indicating ordering tendency

Color changes in CuZn brasses have been observed both with changing composition, hence different phase structures, and on heating [19]. In particular as these alloys are coloured and the changes can be observed visually. A study of the changes in spectral reflectivity due to ordering or segregation would be interesting. The colour of these alloys should be due to the same physical mechanism of internal photoelectric excitations, as proposed for coloured metals like Cu and Au. Of course, we should take care of plasma effects and other phenomena that together and in a combined way give rise to colour. However, it would be, as an initial study, examine the effect of SRO on the spectral reflectivity of the alloy. This is shown in Fig. 10.

The first thing we note that for the completely disordered

alloy the reflectivity has a maximum around $\lambda = 5200 \text{ \AA}$ which is not very different from that of Cu at low temperatures and is in the Yellow-Green region. Below this the reflectivity sharply drops (the reflectivity edge) and light of lower wavelengths is not reflected. With increasing segregation tendency this maximum drops almost linearly with α to around 4950 \AA which is towards the green range. On the other hand with increasing ordering tendency the maximum moves out towards 5600 \AA which moves towards the yellow from the yellow-green wavelengths. We would expect then a shift from a yellow-green colour in the disordered to a more yellow region in the ordered material. We should note that these calculations are all done at 0K. In an actual experiment the disorder-order transition takes place with varying tem-

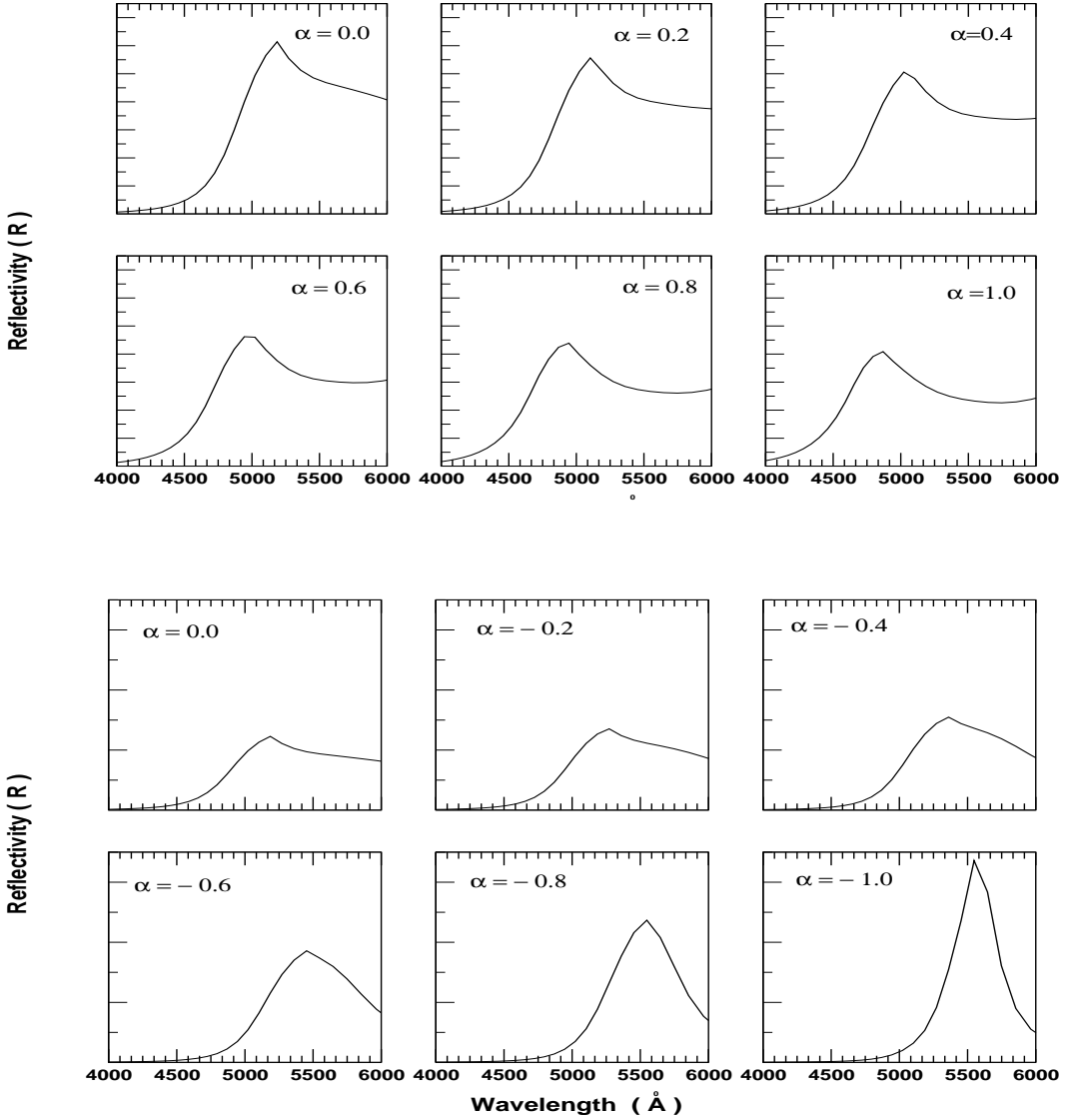


FIG. 10: (Top panel) Reflectivity as a function of the wavelength and its variation with the nearest neighbour Warren-Cowley parameter $\alpha > 0$ increasing indicating segregating tendency. (Bottom panel) The same with $\alpha < 0$ indicating ordering tendency

perature and the temperature effects on the electronic structure must be taken into account, as well as effect of plasma oscillations. We shall leave this for a later communication.

REFERENCES

[1] F. Jona and P.M. Marcus, *J. Phys. Condens Matter* **13** 5507 (2001)
 [2] *Binary alloy phase diagrams* eds. T.B. Massalski, H. Okamoto, P.R. Subramaniam and L. Kacprzak (Materials Park, Ohio : ASM International, 1990)
 [3] W. Hume-Rothery, *The Structure of Metals and Alloys* (London, Institute of Metals, 1936)
 [4] A. Bansil and H. Ehrenreich, *Phys. Rev. B* **9** 445 (1974)
 [5] D.A. Rowlands, J.B. Staunton, B. L. Gyorffy, E. Bruno and B. Ginatempo, *Phys. Rev. B* **72** 045101 (2005)
 [6] M. Jarrell and H. R. Krishnamurthy, *Phys. Rev. B* **63** 125102 (2001)
 [7] F.C. Nix and W. Shockley, *Rev. Mod. Phys.* **10** 1 (1938)
 [8] L. Guttman, in *Solid State Physics* edited by F. Seitz and D. Turnbull (Academic Press Inc., New York, 1956) vol 3
 [9] C.B. Walker and D. T. Keating, *Phys. Rev.* **130** 1726 (1963)
 [10] C.B. Walker and D.R. Chipman, *Phys. Rev. B* **4** 3104 (1971)
 [11] I.A. Abrikosov, A.M.N. Niklasson, S.I. Simak, B. Johans-

son, A.V. Ruban and H.L. Skriver, *Phys. Rev. Lett.* **76** 4203 (1996)

[12] I.A. Abrikosov, Yu. H. Velikov, P.A. Korzhavyi, A.V. Ruban and L.E. Shilkrot, *Solid State Commun* **83** 867 (1992)

[13] D.D. Johnson and F.J. Pinski, *Phys. Rev. B* **48** 11553 (1993)

[14] P.P. Singh, A. Gonis and P.E.A. Turchi, *Phys. Rev. Lett.* **71** 1605 (1993)

[15] P. P. Singh and A. Gonis, *Phys. Rev. B* **49** 1642 (1994)

[16] P.A. Korzhavyi, A.V. Ruban, I.A. Abrikosov and H.L. Skriver, *Phys. Rev. B* **51** 5773 (1995)

[17] Y. Wang, G. Stocks, W.A. Shelton, D.M.C. Nicolson, Z. Szotek and W.M. Temmerman, *Phys. Rev. Lett.* **75** 2867 (1995)

[18] E. Bruno, L. Zingales and A. Milici, *Phys. Rev. B* **66** 245107 (2002)

[19] L. Muldawer, *Phys. Rev.* **127** 1551 (1963)

[20] G. Joos and A. Klopfer, *Z. Physik* **138** 251 (1954)

[21] H. Amar and K.H. Johnson, *Phys. Rev.* **139** A760 (1965)

[22] H. Amar, K.H. Johnson and K.P. Wang, *Phys. Rev.* **148** 672 (1966)

[23] H. Amar, K.H. Johnson and C.B. Sommers, *Phys. Rev.* **153** 655 (1967)

[24] T. Saha, I. Dasgupta and A. Mookerjee, *J. Phys. Condens Matter* **6** L245 (1994).

[25] A. Mookerjee, in *Electronic Structure of Clusters, Surfaces and Alloys* ed. A. Mookerjee and D.D. Sarma (Taylor-Francis, UK) (2003)

[26] A. Mookerjee, *J. Phys. C: Solid State Phys.* **6** 1340 (1973).

[27] T. Kaplan and L. J. Gray, *Phys. Rev. B* **15** 3260 (1977).

[28] T. Saha, I. Dasgupta and A. Mookerjee, *J. Phys. Condens Matter* **8** 1979 (1996).

[29] S. Ghosh, N. Das and A. Mookerjee, *Int. J. Mod. Phys. B* **21** 723 (1999).

[30] I. Dasgupta, T. Saha, A. Mookerjee and G. P. Das, *J. Phys.: Condens. Matter* **9** 3529 (1997).

[31] O. K. Andersen, *Phys. Rev. B* **12** 3060 (1975).

[32] O. K. Andersen and O. Jepsen, *Phys. Rev. Lett.* **53** 2571 (1984).

[33] R. Haydock *Solid State Physics* (Academic Press, New York, 1980), Vol. 35.

[34] N. Beer and D. G. Pettifor, in *The Electronic Structure of Complex Systems*, edited by P. Phariseau and W. M. Temmerman, Vol. 113 of Advanced Study Institute Series B: Physics (Plenum, New York, 1982), p. 769.

[35] R. Haydock, *Philos. Mag. B* **43** 203 (1981); R. Haydock and R. L. Te, *Phys. Rev. B* **49** 10845 (1994).

[36] Haydock R., thesis University of Cambridge, U.K. (1972).

[37] A. Chakrabarty and A. Mookerjee, (2005) *E. Physical J B* **44** 21

[38] A.V. Ruban and H. L. Skriver, *Phys. Rev. B* **66** 024201 (2003)

[39] M. Tsukada, *J. Phys. Soc. Jpn.* **32**, 1475 (1972)

[40] V. Kumar, V.K. Srivastava and A. Mookerjee, *J. Phys. C : Solid State Phys* **15**, 1939 (1982)

[41] A. Mookerjee, *J. Phys. C : Solis State*, **6**, 1340 (1973)

[42] A. Gonis, G.M. Stocks, W.H. Butler and H. Winter, *Phys. Rev. B* **29**, 555 (1984)

[43] L.J. Kaplan and T. Gray, *Phys. Rev. B* **14**, 3462 (1976)

[44] R. Mills and P. Ratanavararaksa, *Phys. Rev. B* **18**, 5291 (1978)

[45] S.S.A. Razee, S.S. Rajput, R. Prasad and A. Mookerjee, *Phys. Rev. B* **42**, 9391 (1990)

[46] A. Mookerjee and R. Prasad, *Phys. Rev. B* **48**, 17724 (1993)

[47] T. Saha, I. Dasgupta and A. Mookerjee, *Phys. Rev. B* **50**, 13267 (1994)

[48] T. Saha, I. Dasgupta and A. Mookerjee, *J. Phys. : Condens. Matter* **8**, 1979 (1996)

[49] A. Chakrabarti and A. Mookerjee, *E. Phys. J. B* **44** 21, (2005)

[50] D. Paudyal, T. Saha-Dasgupta and A. Mookerjee, *J. Phys. : Condens. Matter* **16**, 2317 (2004)

[51] S. Ghosh, P.L. Leath and M.H. Cohen, *Phys. Rev. B* **66**, 214206 (2002)

[52] A. Alam and A. Mookerjee, *Phys. Rev. B* **69**, 024205 (2004)

[53] D.A. Rowlands, J.B. Staunton, B.L. Györffy, *Phys. Rev. B* **67**, 115109 (2003)

[54] D.A. Rowlands, J.B. Staunton, B. L. Györffy, E. Bruno and B. Ginatempo, cond-mat/0411347

[55] K. Tarafder and A. Mookerjee, *J. Phys. Condens Matter* **17** 6435 (2005)

[56] V.S. Viswanath and G. Müller, (1993) in “The user friendly recursion method”, (Troisieme Cycle de la Physique, en Suisse Romande)

[57] D. Hobbs, E. Piparo, R. Girlanda and Monaca M., (1995) *J. Phys. Condens Matter* **7** 2541

[58] K. K. Saha and A. Mookerjee *J. Phys. Condens Matter* **17** 4559 (2005)

[59] K.K. Saha, A. Mookerjee and O.Jepsen, *Phys. Rev. B* **71** 094207 (2005)